Dielectric properties of Si–$Ba_{0.5}Sr_{0.5}TiO_3$ composite thin films elaborated by pulsed laser deposition

L. Z. Cao, B. L. Cheng,[a] S. Y. Wang, Y. L. Zhou, K. J. Jin, H. B. Lu, Z. H. Chen, and G. Z. Yang

Beijing National Laboratory for Condensed Matter Physics, Institute of Physics, Chinese Academy of Sciences, Beijing 100080, China

(Received 13 April 2005; accepted 22 June 2005; published online 9 August 2005)

Si–$Ba_{0.5}Sr_{0.5}TiO_3$ composite thin films were deposited by pulsed laser deposition technique on (100) Nb:$SrTiO_3$ substrates. The crystal structure and surface morphology of the thin films have been characterized by x-ray diffraction and atomic force microscopy, respectively. Experimental results suggested that the Si composition has played a positive role in improving the dielectric properties of the thin films. With the increased Si concentration, the dielectric loss was significantly reduced, accompanied with a tolerable reduction of tunability. In particular, the 14% Si composite film exhibited a dielectric loss of 0.005, which is much lower than that of the undoped $Ba_{0.5}Sr_{0.5}TiO_3$ (BST) film. Moreover, a proper concentration of Si in the film improved the figure of merit from 9 of the undoped BST to 23 of 1.4% Si composite films. © *2005 American Institute of Physics*. [DOI: 10.1063/1.1999852]

I. INTRODUCTION

Because high dielectric susceptibility is easily tuned by an electric field, $Ba_xSr_{1-x}TiO_3$ (BST) thin films are suitable for use in agile microwave devices such as filter, phase shifter, and antenna. In practical tunable device applications, several critical requirements should be satisfied, which include low dielectric loss, adequate tunability, low leakage current, permittivity of less than 500, and so on.[1] It is well known that the modified properties of the $Ba_xSr_{1-x}TiO_3$ thin film can be obtained by means of a small concentration of dopants. So far, many kinds of materials have been successfully introduced as dopants to improve its electric and dielectric properties, such as Mg, La, Au, Al_2O_3, Co, Mn, Bi, etc.[2–9] One possible mechanism to explain the improvement is that ions with a charge less than 4+ can substitute for the *B* sites of the ($A^{2+}B^{4+}O_3^{2-}$) perovskite structure and behave as electron acceptors, which prevent the reduction of Ti^{4+} to Ti^{3+} by neutralizing the donor action of the oxygen vacancies.[1] Another mechanism is that the oxygen vacancies in the films can be reduced by an additional supply of a more reactive atomic oxygen.[10] For example, Srivastava *et al.* reported that atomic oxygen generated from the dissociation of metastable AgO easily bonded to the cations in BST, resulting in the reduction of the oxygen vacancies, which consequently improved the dielectric properties of Ag-doped BST thin films.[11] Moreover, the greatly decreased loss of a $Ba_{0.6}Sr_{0.4}TiO_3$ thin film has been obtained by using a thin film of SiO_2 dielectric barrier, but the tunability dropped sharply, which prevented it from practical use.[12] In order to solve the problem, we use Si composition to optimize the dielectric properties of a $Ba_{0.5}Sr_{0.5}TiO_3$ thin film. In this paper, we systematically investigate the dielectric properties of Si–$Ba_{0.5}Sr_{0.5}TiO_3$ (Si–BST) composite thin films with the concentration of Si from 1.4% to 14%. It is shown that the Si–BST composite thin films have low loss and tolerably decreased tunability with the proper concentration of Si composition.

II. EXPERIMENTS

A conventional ceramic processing was used to prepare the BST target for pulsed laser deposition (PLD). $BaCO_3$, $SrCO_3$, and TiO_2 powers were mixed in stoichiometric proportion and first calcinated at 800 °C for 10 h in atmosphere. After sufficiently crushing and mixing the resultant powder for 1 h, the BST target with a diameter of 25 mm was compacted and sintered at 1300 °C for 10 h. The PLD experiment was performed using a XeCl excimer laser system with a repetition rate of 3 Hz and an average pulse energy of 240 mJ. The deposition of the Si–BST composite film was carried out at a substrate temperature of 650 °C with an oxygen pressure of 1 Pa. The concentration of Si in the BST thin film was controlled through changing the coverage area of Si pieces over the BST target surface, as shown in Fig. 1.

FIG. 1. Schematic configuration of the Si–BST target controlling the Si concentration in the thin film.

[a]Author to whom correspondence should be addressed; electronic mail: blcheng@aphy.iphy.ac.cn

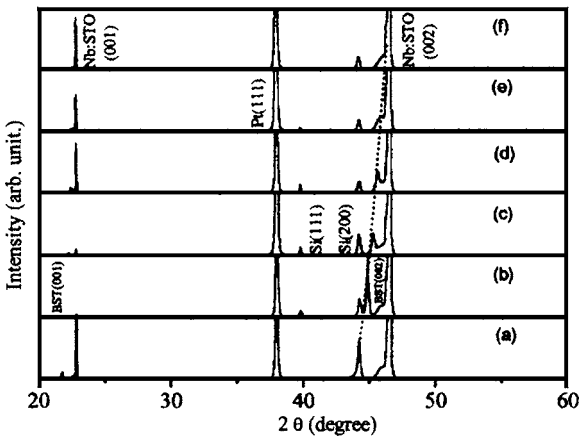

FIG. 2. XRD patterns of the thin films on Nb:STO substrates: (a) undoped BST, (b) Si(5)–BST, (c) Si(10)–BST, (d) Si(20)–BST, (e) Si(30)–BST, and (f) Si(50)–BST.

The films deposited with the θ angle of 5°, 10°, 20°, 30°, and 50° were noted as Si(5)–BST, Si(10)–BST, Si(20)–BST, Si(30)–BST, and Si(50)–BST, respectively. The target and $Nb:SrTiO_3$ (STO) substrate with (100) orientation were positioned parallel, with a 50-mm separation. After the deposition of the BST thin film, Pt top electrodes were deposited through a shadow mask on the BST thin films under the pressure of 1×10^{-3} Pa at room temperature. Then the samples were rapid thermal annealed (RTA) at 600 °C for 10 min, which has been proven to be necessary to obtain low leakage current and also to improve the top electrode/BST contact.[13] Thus, parallel-plate capacitors were fabricated for the dielectric property investigation of the Si–BST composite thin film.

The film thickness was measured around 370 nm by a surface profiler of Dektak 8. The crystal structure of the Si–BST composite thin films was determined by x-ray diffraction (XRD) using Cu $K\alpha$ radiation with a wavelength of 1.5405 nm. The surface morphologies of the films were observed with a Nanoscope IIIa-D3000 atomic force microscope (AFM). The dielectric properties of the Si–BST composite thin film in terms of permittivity (ε_r) and dielectric loss ($\tan\delta$) were measured by an Agilent 4294A precision impedance analyzer at room temperature.

III. RESULTS AND DISCUSSION

The XRD patterns of the films are plotted in Fig. 2. It can be seen that all the films have a phase of perovskite structure. With increased Si concentration, the diffraction peaks ($k00$) for the BST shift to high angles as shown in Fig. 2, which indicates a decrease of the lattice parameter because the Si^{4+} ion with a small radius of 0.54 Å replaces the Ti^{4+} ion with a large radius of 0.745 Å. Furthermore, the intensity of the (200) peak decreases and the full width at half maximum (FWHM) of the peak increases gradually, which may be connected to the decreased crystallization and the increased Si concentration. For the Si–BST composite films, two peaks are observed at 39.78° and 44.24°, which are caused by a second phase of excessive Si content. As demonstrated by the XRD results, a portion of Si ions is incorporated into the BST lattice, and another portion of Si is formed as a second phase in the thin films. Therefore, Si–BST composite thin films are elaborated.

The surface morphologies of the films are shown in Fig. 3. It is found that both the undoped and Si–BST composite films exhibit a root-mean-square surface roughness (R_{rms}) of less than 3.2 nm. With increased Si concentration, the thin films show a trend of improved surface morphologies (not shown in Fig. 3).

The permittivity ε_r of the Si–BST composite films as a function of the applied electric field is shown in Fig. 4. The permittivities at zero-bias electric field are 805, 865, 460, 357, 222, and 68 for the undoped BST, Si(5)–BST, Si(10)–BST, Si(20)–BST, Si(30)–BST, and Si(50)–BST, respectively. Most of the Si–BST composite films exhibit lower permittivities than that of the undoped one, except for the Si(5)–BST which has the highest permittivity of 865. Similar phenomena were also observed in Ni-doped $Ba_{0.5}Sr_{0.5}TiO_3$ thin films.[14] Jeon *et al.* reported that the permittivity of a Ni-doped BST thin film increased with increased Ni-dopant concentration of up to 3 mol %, and when the concentration was above 3 mol %, the permittivity decreased slightly. However, the exact mechanism by which the Si composition changes the dielectric properties requires further investigation. From the XRD patterns, we observe that the Si(5)–BST

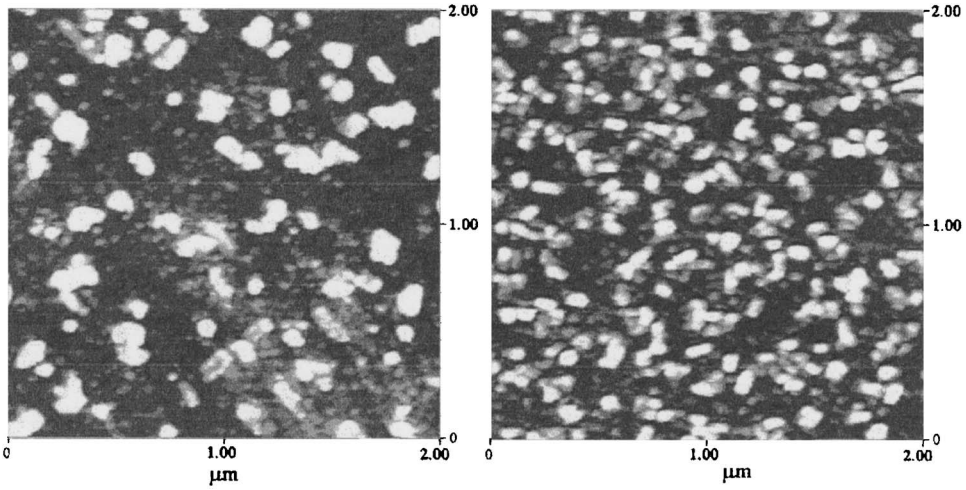

FIG. 3. AFM micrographs of surface morphology: (a) undoped BST film and (b) Si(20)–BST thin film.

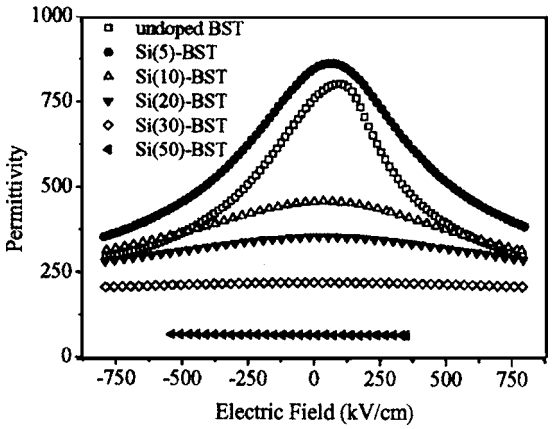

FIG. 4. Permittivity as a function of the electric field in the range from −800 to 800 kV/cm.

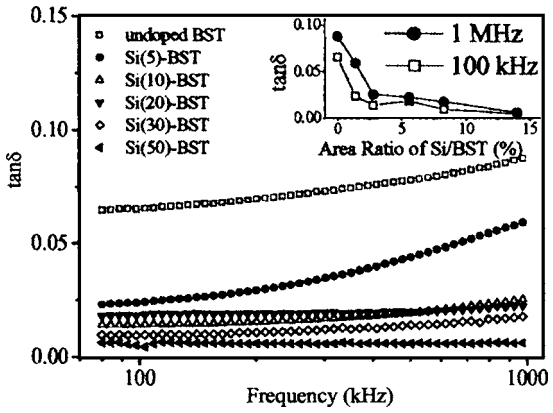

FIG. 5. Dielectric loss as a function of frequency for undoped and Si–BST composite thin films.

film has the most intensive (200) peak, which indicates the best crystallization of the film, corresponding to the highest permittivity.

Now, we try to understand the variation of permittivity as a function of Si concentration. Because the decrease in permittivity has been observed with the increase in Si concentration, as a simple hypothesis, we suppose that there was a two-layer structure, in which a capacitor of Si is in series with a capacitor of BST. Then, the permittivity of the Si-BST composite film can be calculated from the formula

$$\frac{1}{C} = \frac{1}{C_{\mathrm{Si}}} + \frac{1}{C_{\mathrm{BST}}}, \tag{1}$$

which means

$$\frac{d}{\varepsilon_r} = \frac{d_{\mathrm{Si}}}{\varepsilon_{\mathrm{Si}}} + \frac{d_{\mathrm{BST}}}{\varepsilon_{\mathrm{BST}}}, \tag{2}$$

where d is the total thickness of the Si–BST composite thin film; d_{Si} and d_{BST} are the thickness of the Si and BST capacitors, which were calculated from the coverage ratio of Si and BST on the target, respectively; ε_r is the permittivity of the film; $\varepsilon_{\mathrm{Si}}$ is the permittivity of the Si which is 11.9;[15] and $\varepsilon_{\mathrm{BST}}$ is the permittivity of the undoped BST film in our experiment, which is 805. The ε_r calculated from Eq. (2) are 416, 280, 171, 122, and 78 for the Si(5)–BST, Si(10)–BST, Si(20)–BST, Si(30)–BST, and Si(50)–BST thin films, respectively, which exhibit a similar trend to the result of the experiment. As a simple hypothesis, it only provides us a probable trend and the exact mechanism needs further research. On the other hand, we observe the similar trend of the intensity of the (200) peak with the increase in the Si content in the XRD patterns in Fig. 2.

It is known that a tunable microwave device requires a high dielectric tunability and a low dielectric loss. The dielectric tunability is calculated from the formula

$$\text{Tunability} = \frac{\varepsilon(0) - \varepsilon(E_{\max})}{\varepsilon(0)}, \tag{3}$$

where $\varepsilon(0)$ and $\varepsilon(E_{\max})$ represent the permittivities at zero applied electric field and at maximum applied electric field, respectively. The tunability, measured at 800 kV/cm, is found to decrease monotonically as a function of increased Si concentration. The most interesting feature is that the Si–BST composite films maintain a tolerable tunability with the decreased dielectric loss. However, due to the high leakage current, the film of Si(50)–BST was only measured in the range from −550 to 300 kV/cm.

From the results shown in Fig. 4, it is evident that the permittivities of the films decrease with the increase in the electric field. The nonlinearity of permittivity with electric field at the paraelectric phase of the BST film results from the anharmonic interaction of titanium ions in the perovskite structure;[2] ε_r as a function of the electric field can be interpreted by a theory proposed by Johnson,[16,17] which can be represented as

$$\varepsilon_r/\varepsilon_{r0} = 1/(1 + \eta\varepsilon_{r0}^3 E^2)^{1/3}, \tag{4}$$

where ε_{r0} and ε_r are the permittivities under a zero electric field and under an electric field E, respectively, and η is the phenomenological coefficient.

The dielectric loss as a function of frequency measured at room temperature is given in Fig. 5. As shown in the inset of Fig. 5, with the increase in Si concentration noted as Si/BST area ratio, the dielectric loss of BST thin films reduces obviously. The tan δ of the thin films are 0.066, 0.024, 0.014, 0.018, 0.010, and 0.005, corresponding to undoped BST, Si(5)–BST, Si(10)–BST, Si(20)–BST, Si(30)–BST, and Si(50)–BST, respectively. In other words, the lowest tan δ of 0.005 corresponds to a 14% Si/BST area ratio.

It was proposed that the electron hopping resulting from the generation of oxygen vacancy between different titanium ions provides a mechanism for dielectric loss.[1,18] In our experiments, the decrease in dielectric loss can be attributed to the steady valence of Si^{+4} ions, which reduces the hopping of electrons from Ti^{+4} to Ti^{+3}. On the other hand, the improved surface roughness observed in the AFM patterns may play a positive role in the decrease in dielectric loss, which ensures excellent adhesion with the Pt electrodes in the Nb:STO/BST/Pt structure.

There is inevitably a trade-off for the application because the reduction of the dielectric loss usually accompanies the reduction of dielectric tunability. In a tunable microwave device, the figure of merit K is usually used to evaluate

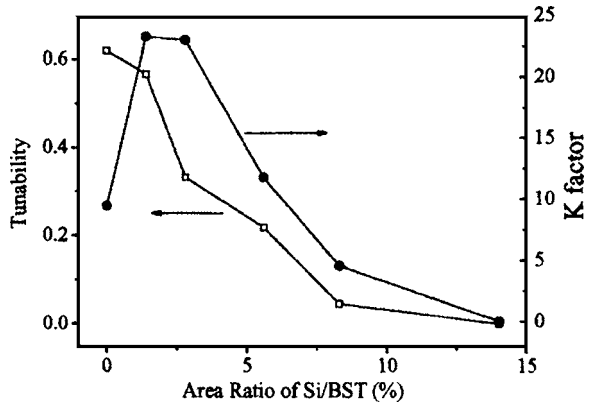

FIG. 6. Tunability and *K* factor as a function of Si concentration at a frequency of 100 kHz.

the quality of ferroelectric films, which is defined by taking into consideration the dielectric loss and tunability as follows:

$$K = \left(\frac{\text{Tunability}}{\tan\delta}\right) = \left\{\frac{[\varepsilon(0) - \varepsilon(E_{\max})]/\varepsilon(0)}{\tan\delta}\right\}. \quad (5)$$

The tunability and *K* factor as a function of Si concentration are shown in Fig. 6 and Table I. It is found that a maximum *K* factor of 23 obtained in the low Si concentration [Si(5)–BST], i.e., 1.4% Si, thin film is much higher than that of the undoped BST thin film due to a small decreased tunability. This experimental result shows a better dielectric property behavior than that in BST(6:4) thin films with a SiO_2 buffer layer[12] and demonstrates an attractive prospect for the tunable microwave device application.

TABLE I. Summary of dielectric properties of Si–BST composite thin films.

Films	ε_r	$\tan\delta$ (100 kHz)	Dielectric tunability (% for 800 kV/cm)	*K* factor
Undoped BST	805	0.065	62	9
Si(5)–BST	865	0.024	57	23
Si(10)–BST	460	0.014	33	22
Si(20)–BST	357	0.018	22	11
Si(30)–BST	222	0.010	5	5
Si(50)–BST	68	0.005	0[a]	0

[a]Measured in the range from −550 to 300 kV/cm because of the high leakage current.

IV. CONCLUSIONS

Our experimental results demonstrate that *c*-axis-oriented Si-BST composite films can be elaborated on a (100) Nb:STO substrate by a PLD technique. The microstructure and dielectric properties have been studied systemically. The XRD patterns show that a portion of the Si ions is incorporated into the BST lattice and another portion of Si is formed as the second phase in the thin films. The incorporation of Si significantly influences the dielectric properties of the BST thin film. The dielectric loss has been reduced from 0.06 (undoped BST) to 0.005 [Si(50)–BST], and the figure of merit has been increased from 9 (undoped BST) to 23 [Si(5)–BST]. It suggests that such a Si–BST composite thin film is practically significant from the viewpoint of the requirement of microwave device application.

ACKNOWLEDGMENT

The authors are very grateful for the financial support of the National Natural Science Foundation of China.

[1]M. W. Cole, P. C. Joshi, and M. H. Ervin, J. Appl. Phys. **89**, 6336 (2001).
[2]P. C. Joshi and M. W. Cole, Appl. Phys. Lett. **77**, 289 (2000).
[3]M. W. Cole, W. D. Nothwang, C. Hubbard, E. Ngo, and M. Ervin, J. Appl. Phys. **93**, 9218 (2003).
[4]H. W. Wang, S. W. Nien, and K. C. Lee, Appl. Phys. Lett. **84**, 2874 (2004).
[5]K. B. Chong, L. B. Kong, L. F. Chen, L. Yan, C. Y. Tan, T. Yang, C. K. Ong, and T. Osipowicz, J. Appl. Phys. **95**, 1416 (2004).
[6]S. Y. Wang, B. L. Cheng, C. Wang, S. Y. Dai, H. B. Lu, Y. L. Zhou, Z. H. Chen, and G. Z. Yang, Appl. Phys. Lett. **84**, 4116 (2004).
[7]S. Y. Wang, B. L. Cheng, C. Wang, H. B. Lu, Y. L. Zhou, Z. H. Chen, and G. Z. Yang, J. Cryst. Growth **259**, 137 (2003).
[8]H. D. Wu and F. S. Barnes, Integr. Ferroelectr. **22**, 291 (1998).
[9]K. T. Kim and C. L. Kim, Microelectron. Eng. **66**, 835 (2003).
[10]K. P. Jayadevan, C. Y. Liu, and T. Y. Tseng, Appl. Phys. Lett. **85**, 1211 (2004).
[11]A. Srivastava, D. Kumar, and R. K. Singh, Phys. Rev. B **61**, 7305 (2000).
[12]V. Reymond, D. Michau, S. Payan, and M. Maglione, Ceram. Int. **30**, 1085 (2004).
[13]Y. D. Xia, D. Wu, and Z. G. Liu, J. Phys. D **37**, 2256 (2004).
[14]Y. A. Jeon, T. Suck, and S. G. Yoon, Jpn. J. Appl. Phys., Part 1 **40**, 6496 (2001).
[15]S. M. Sze, *Physics of Semiconductor Devices* (Wiley-Interscience, New York, 1981), p. 849.
[16]L. Wu, Y. C. Chen, Y. T. Tsai, and S. Y. Chu, Jpn. J. Appl. Phys., Part 1 **38**, 5154 (1999).
[17]K. M. Johnson, J. Appl. Phys. **33**, 2826 (1961).
[18]X. X. Xi, H. C. Li, W. D. Si, A. A. Sirenko, I. A. Akimov, J. R. Fox, A. M. Clark, and J. H. Hao, J. Electroceram. **4**, 393 (2000).